SMALL CRAFT NOISE: INFLUENCE OF SPEED AND RUNNING ATTITUDE ON RADIATED NOISE LEVELS

L G M Star	BMT, 70 Victoria Street, London, SW1E 6SQ
T A Smith	Dept. Mechanical Engineering, University College London
A Grech La Rosa	Dept. Mechanical Engineering, University College London

1 INTRODUCTION

For many large commercial vessels there is now a wealth of data showing a positive correlation between speed and underwater noise[1]. There has been an interest in the anthropogenic underwater noise created by large commercial vessels for a long time[2] and there is now a significant body of research into ways of reducing URN from large vessels[3]. Merchant ships have been found to elevate the ambient noise levels by 20 - 30 dB in many areas[1]. However, for small vessels the picture is more nuanced, and some studies have shown that small craft can be noisier at lower speeds due to nonlinear changes in engine and propeller loading, and running attitude across their speed profiles. Firstly, despite their reduced size, these smaller vessels do not necessarily produce less underwater noise (source levels in excess of 170 dB re 1 μ m are reported)[4] and such vessels could be more likely to come into contact with wildlife in rich, biodiverse coastal waters[5].

In this work, the results of trials conducted on two small vessels (a pilot boat and a RIB) are presented across a broad range of speeds. The aim is to characterise the noise levels and provide an understanding of how they vary with speed. Hydrophone measurements are combined with data from vibration sensors to provide a more complete understanding of the noise sources and how they vary with speed.

2 METHODS

2.1 Trial Location and Vessel Descriptions

The trials were conducted in Bigbury Bay, South Devon over a two-day period from 7th to 8th July 2023. An echo sounder was used to measure the water depth of the trial area; the average depth was recorded as 27m. The bathymetry of the trial area was found to show a gradual increase in the depth from the shoreline to the trial route. Seabed samples were taken which found the upper layer to be a mixture of sand and mud. An AIS receiver was used to monitor local marine traffic throughout the trials. No other vessels were identified within 5km of the trial area or visible during the trials. The weather, based on forecast data and observations was Beaufort 4 and upper sea state 3.

Two vessels were used in the trials: a pilot boat (PB) and a rigid inflatable boat (RIB). The vessels were chosen to provide a good representation of the type of small craft vessels which are popularly used.

The principal particulars of the two vessels are given in Table 1.

Table 1: Principal particulars of the trial vessels

	Pilot Boat	**RIB**
Length overall (m)	9.9	7.2
Beam (m)	3.5	2.6
Static draught (m)	0.6	0.35
Max engine power (kW)	2 x 177	129
Max shaft speed (rpm)	3300	5500-6100

The pilot boat size, design and propulsion architecture was quite typical of many small fishing vessels, support vessels and leisure vessels. It was powered by twin inboard diesel engines and twin shafts with 4-bladed propellers. The engines were 4-stroke and had 4 cylinders. The maximum speed achieved by the pilot boat during the trial conditions was 16 knots. RIBs are widely used around the world and have a relatively common design with hard-chine hullforms and outboard engines. The RIB used had a single 4-stroke petrol outboard engine with a 3-bladed propeller. The maximum speed achieved by the RIB during the trial conditions was 26 knots.

2.2 Experimental Methods

For this trial, the terminology in ISO18405 (2017)[6] was used, and much of the methodology follows that set out in ISO17208-1 (2016)[7]; ISO17208-2 (2019)[8]. The experimental methodology deviates from the ISO standards in matters of water depth and calculating the propagation losses. To measure the underwater radiated noise of each vessel, the small craft were assessed at multiple speeds, as shown in Table 2, within a given trial area. For each trial run, as shown in Figure 1, the vessel being assessed travelled 500m in a straight line from the COMEX to the FINEX points. The vessel achieved the desired speed before commencing a run and the speed was then kept as constant as possible during the run. The data window length (DWL) used for the subsequent analysis of the noise levels was 100m. At least two double runs were conducted for each speed. GPS onboard both vessels was used to monitor the speed and location throughout the trials.

Table 2: Speeds assessed for each vessel

Vessel	**Speeds assessed (knots)**
Pilot Boat	6,10,14,16
RIB	6,10,14,18,22,26

Four RS Aqua/Turbulent Research Porpoise acoustic recorders were used for capturing the underwater noise measurements in the trial. The hydrophones were arranged in two vertical arrays, denoted $R_{1a,b}$ and $R_{2a,b}$, at 40 m and 85 m from the closest point of approach (CPA), as shown in Figure 1. Two hydrophones were placed at each distance to account for spatial variability in the acoustic field and to reduce the uncertainty in the results. The arrays were held in place by weights, with floats used to keep the lines taut and prevent movement.

Piezoelectric accelerometers were mounted onboard the vessels to measure the hull vibration across

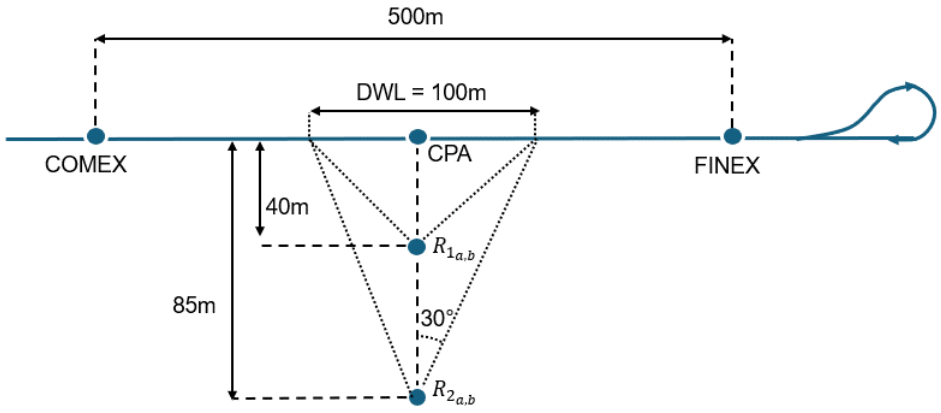

Figure 1: Schematic showing how the trials were conducted.

a frequency range of 10 - 8000 Hz. For the pilot boat, the vibration sensors were placed in two distinct locations: inside of the hull close to the bow and mounted on the deck at the transom. The RIB had one set of vibration sensors placed inside of the hull at midships. The vibration measurements were used to provide insight into the relationship between vessel speed, vibration and underwater noise. The shaft speed was recorded for both vessels during the trials which enabled the cylinder firing rate (C), engine firing rate (E) and blade passing frequency (B) to be determined.

Both vessel engines are 4-stroke and have 4 cylinders, for a given shaft speed of N rpm, the cylinder and engine firing rates and their harmonics are given by

$$C = \frac{Ni}{120}, i = 1, 2, ... \tag{1}$$

$$E = 4Ci, i = 1, 2, ... \tag{2}$$

The blade passing frequency and harmonics are

$$B = \frac{Nzi}{60g}, i = 1, 2, ... \tag{3}$$

where g is the gearbox ratio and z is the number of propeller blades.

2.3 Source Level Calculation

The source levels for both vessels can be estimated from the measured levels recorded by each hydrophone and accounting for propagation loss. In shallow water, the material composition of the seabed can alter the reflectivity of the waves and affect the propagation losses experienced and add complexity to the acoustic field. The Lloyd's Mirror Effect is often amplified on small vessels due to a shallower draught leading the acoustic source to be closer to the surface. A detailed comparison of the analytical approaches to propagation loss can be found in Meyer and Audoly, 2022[9]. The Seabed Critical Angle Method (SCA) was developed to account for both the seabed and sea surface effects by MacGillivray et al., 2023[10].

2.3.1 Determination of Propagation Losses

To determine the validity of the SCA approach for the trial conditions, the two hydrophone arrays are used to compute the transmission loss between array 1 (40m) and array 2 (85m) for different trial runs. Firstly, the results are compared to background noise measurements to determine the validity of a given run. The approach set out in ISO 17208-1[7] for correcting or discarding a particular dataset is applied. For a given decidecade band, if the background noise, L_{pn}, is at least 10 dB lower than that from a trial run, L_{ps+n}, no correction is made. If the background noise is within 3 dB of the trial run, the run is discarded. If $3 \leq L_{ps+n} - L_{pn} \leq 8$, then the background noise is subtracted from the trial data. Once any corrections are made to the trial data, the difference between the two distances can be calculated for each speed and averaged. The frequency dependent coefficient, A(f), can then be obtained from the difference in the formula which enables the overall propagation loss from the source to be estimated,

$$\mathsf{TL}_{\mathsf{exp}} = A(f) \log_{10}\left(\frac{r}{r_0}\right) \tag{4}$$

Figure 2 shows the experimentally derived propagation losses from the source to hydrophone R_{1a} for the RIB travelling at 22 and 26 knots. The curves are shown alongside the SCA method with an ISO 17208[8] recommended source depth of 0.24m. There is generally a good agreement between the analytical and experimental approaches.

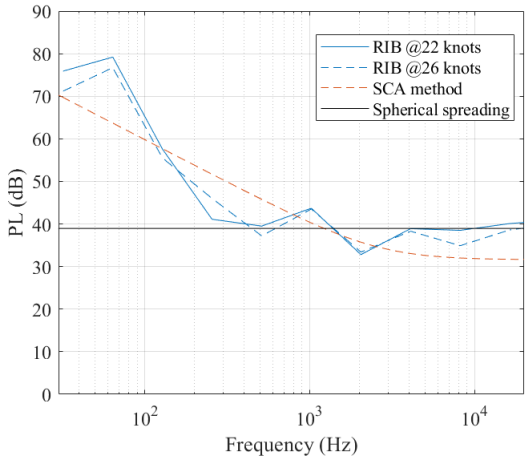

Figure 2: Experimental and analytical propagation losses for CPA = 85m.

3 RESULTS

3.1 Source Levels for the Pilot Boat and RIB

The overall source levels, $L_{S,OA}$, for both vessels across their speed ranges are shown in Figure 3. These have been generated by integrating the power spectral densities over 10 - 20000 H_z. For the pilot boat, the overall source levels increase significantly with speed: from 156 dB at 6 knots to 173 dB at 16 knots. This contrasts sharply with the RIB where the source levels only vary by 2 dB across the entire speed range. The source levels seem unusual as vessel noise typically increases with speed but Picculin et al[4]

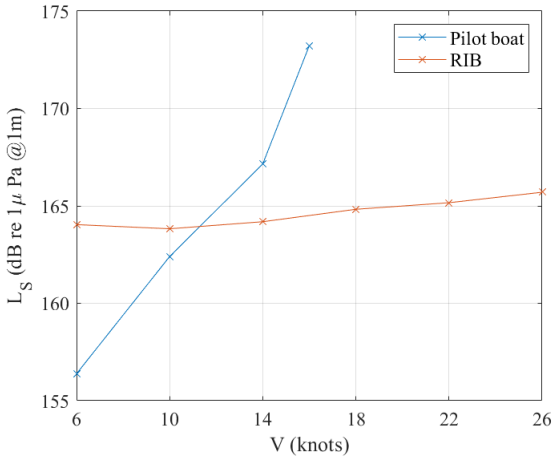

Figure 3: Overall source levels for the pilot boat and RIB as a function of speed

have also reported similar behaviour for a RIB. In their study they found that a similar sized RIB showed only a 2 dB increase in the source level across a speed increase of 10 knots.

Further insights can be gained by looking at the decidecade band data for the two vessels, shown in Figure 4. The source levels for the pilot boat are dominated by low frequency sound. As the speed of the pilot boat increases, the frequency of the dominant sources at $60 \leq f \leq 100Hz$ increases due to a greater shaft speed. The higher frequencies also show an increase in broadband noise with speed and a scaling of sound level with speed to the power 6 is noted here. The relationship between the source levels and speed for the RIB is more complex. The source levels are still dominated by lower frequency sound but do not show a notable increase with speed. There is a high frequency component at 4 kHz that increases with speed but is not a dominant source.

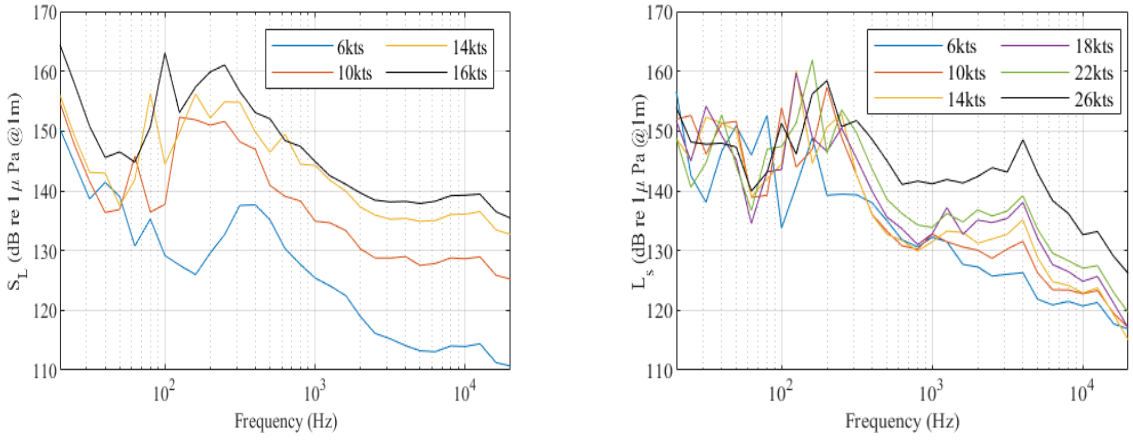

(a) ***(b)***

Figure 4: Decidecade band source levels for (a) pilot boat and (b) RIB at multiple speeds.

3.2 Narrowband Analysis

Narrowband analysis has been performed for both vessels for frequencies up to 1 kHz. This is shown in Figure 5 for the pilot boat at 16 knots and in Figure 6 for the RIB at 26 knots. A bin width of 1 Hz is used in these figures. The shaft speeds recorded during each trial have been used to determine the cylinder and engine firing rates and blade passing frequencies which have been compared with the tonal peaks for both vessels.

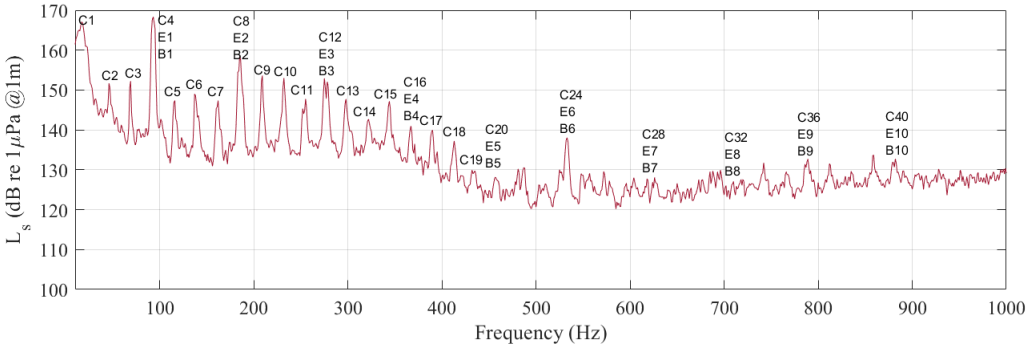

Figure 5: Narrowband acoustic spectra for the pilot boat at 16 knots. The cylinder firing rates are denoted C, engine firing rate, E, and propeller blade rate B.

For the pilot boat, the propeller blade rate (denoted B) is equal to the engine firing rate (E) as a result of the propulsion arrangement. This leads to a series of prominent, equally spaced tonal components at multiples of the cylinder firing rate (C) because $E_i = B_i = 4C_i$ for the i^{th} harmonic. Every prominent tonal component in the spectrum lines up with the cylinder firing harmonics, which shows that the low frequency noise is almost completely due to the cylinder firing processes and the blade rate harmonics. Unfortunately, due to the matching of the engine and propeller frequencies, it has not been possible to determine the dominant contributor. The tones are wider than expected which is due to the pilot boat operating under a varying load.

For the RIB, the low frequency noise is dominated by the engine. The RIB propeller operates in a different flow regime to the pilot boat. Spatial variations in the wake, as a result of the strut on the engine and flow over the bottom of the hull, that lead to prominent blade rate harmonics are reduced for the RIB.

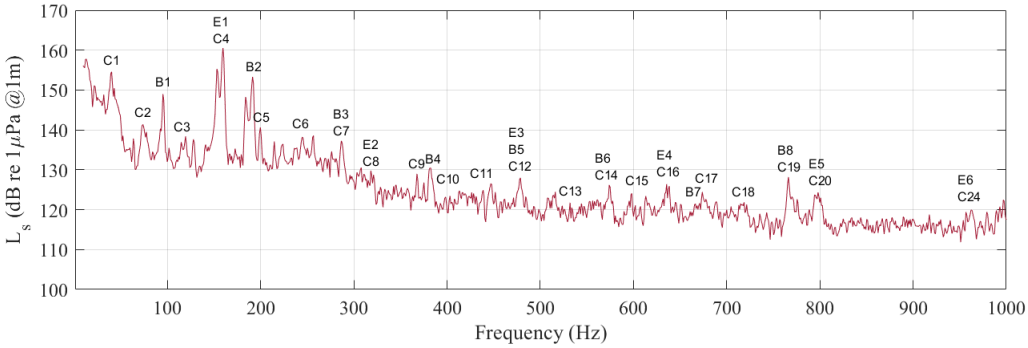

Figure 6: Narrowband acoustic spectra for the RIB at 26 knots. The cylinder firing rates are denoted C, engine firing rate, E, and propeller blade rate B.

3.3 Effect of Running Attitude

The RIB only showing a small increase in source levels with speed warrants further investigation. Vibration data presented in Figure 7 show the decidecade band vibration levels measured on the inside of the RIB hull. There is a significant increase in the vibration levels at all measured frequencies as the speed increases, something which is not reflected in the acoustic data in Figure 3. The greatest increase in vibration levels is seen between 6 knots and 14 knots. There is a clear increase in vibration levels associated with the engine that do not translate into increases in the underwater radiated noise. To understand why this happens, we must look at the running attitude of the vessel which can be explained using the Froude number $F_n = V_m/\sqrt{gL_{wl}}$ where V_m is the vessel speed in ms^{-1} , g = 9.81 ms^{-2}, and L_{wl} is the waterline length. The RIB is a planing vessel, and at 6 knots F_n = 0.39. At this Froude number, the vessel is beginning to lift out of the water and encounters a sharp rise in resistance for $0.3 \leq F_n \leq 0.6$, which results in increased engine and propeller loading and explains the increase seen in vibration levels between the slower speeds. We would expect the RIB to begin planing at around $F_n \approx 1.0$[11], corresponding to a speed of 15.5 knots but based on the trials the vessel actually started to plane at around 14 knots. There are two reasons why the increase in vibration does not translate into an increase in underwater noise. The first is a result of the Lloyd's Mirror Effect. As the vessel speed increases, it lifts out of the water, the source depth decreases and the propagation losses increase. The second is that the engine vibrations are transmitted via the hull and as the vessel starts to plane the percentage of vibration transmitted via the hull decreases. An increase in vibration levels for a planing vessel does not directly translate to an increase in underwater noise.

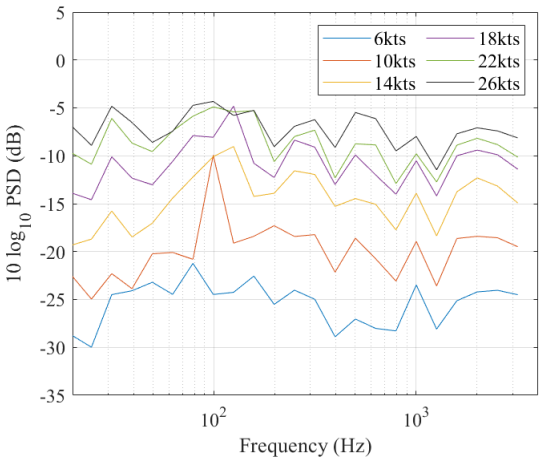

Figure 7: Power spectral densities of the vibration levels (measured as vertical acceleration) inside the hull on the RIB

4 CONCLUSION

This paper has presented results from acoustic trials conducted on two small vessels (a pilot boat and a RIB) across a broad range of speeds in shallow water. The source levels of the pilot boat increased significantly across the speed range (6 to 16 knots), whilst the levels for the RIB remained fairly constant across a broader speed range (6 to 26 knots). The noise from the pilot boat was dominated by tonal noise from the engine and propeller and increases significantly as a function of speed. This was likely made worse by the engine and propeller harmonics being at the same frequencies. Whilst design practice for

larger vessels should avoid these frequencies lining up, such guidance is often not considered in small boat design. This can lead to such craft having unnecessarily high source levels and it would be of interest to see how following best practice more closely could reduce the source levels. The low frequency noise from the RIB is dominated by the engine noise across the speed range, even at higher speeds. This is most likely due to two factors. Firstly, the engine is directly mounted to a lightweight hull, which acts as an effective transmitter of the engine noise into the water. Secondly, because the propeller is located below the hull it operates in flow with less spatial variation than the propellers behind the pilot boat. This reduces the amplitude of the blade rate noise, reducing the overall contribution of the propeller noise. It has also been shown that, despite the onboard vibration levels increasing significantly with speed, this does not translate into significant increases in radiated noise. This can be explained by considering the running attitude of the vessel. As the speed increases, the vessel lifts out of the water and planes, thus reducing the transmission efficiency of the engine noise into the water. Further results and analysis from these trials can be found in [12].

ACKNOWLEDGMENTS

The authors would like to thank Hock An Low, Chang-Yi Tong, Chia-Hsing Yang and Karthiyalini Senthilnathnan, Jake Rigby, Bill Wood and Sea Regs Training School.

REFERENCES

1. P T Arveson and D J. Vendittis. Radiated noise characteristics of a modern cargo ship. *The Journal of Acoustical Society of America*, 107(1):118–129, 2000.
2. J A. Hildebrand. Anthropogenic and natural sources of ambient noise in the ocean. *Marine Ecology Progress Series*, 395:5–20, 2009.
3. T A Smith and J Rigby. Underwater radiated noise from marine vessels: A review of noise reduction methods and technology. *Ocean Engineering*, 266:112863, 2022.
4. M Picciulin, E Armelloni, R Falkner, N Rako-Gospić, M Radulović, G Pleslić, S Muslin, H Mihanović, and T. Gaggero. Characterization of the underwater noise produced by recreational and small fishing boats less than 14m in the shallow-water of the cres-lošinj natura 2000 sci. *Marine Pollution Bulletin*, 183, 2023.
5. WWF. https://www.wwf.org.uk/sites/default/files/2020-01/our planet ourseas.pdf.
6. ISO18405. Underwater acoustics - terminology. 2017.
7. ISO17208-1. Underwater acoustics - quantities and procedures for description and measurement of underwater sound from ships. part 1: Requirements for precise measurements in deep water used for comparison purposes. 2016.
8. ISO17208-2. Underwater acoustics - quantities and procedures for description and measurement of underwater sound from ships. part 2: Determination of source levels from deep water measurements. 2019.
9. V Meyer and C. Audoly. On empirical formulae to assess the source level of ships in shallow water with different hydrophone configurations. *Proceedings on Meetings on Acoustics*, 2022.
10. A O MacGillivray, S B Martin, M A Ainslie, J N Dolman, Z Li, and G A Warner. Measuring vessel underwater radiated noise in shallow water. *The Journal of the Acoustical Society of America*, 153(3):1506–1524, 2023.
11. A.F Molland, S.R Turnock, and D.A. Hudson. *Ship resistance and propulsion*. Cambridge University Press, 2017.
12. T A Smith, A Grech La Rosa, and B Wood. Underwater radiated noise from small craft in shallow water: Effects of speed and running attitude. *Ocean Engineering*, 306:118040, 2024.